
The ageing of colloidal gels induced by Critical Casimir forces

Stephan Kok, 10627978

Report Bachelor Project Physics and Astronomy 15 EC
conducted between 27-03-2016 and 12-07-2016

University of Amsterdam, Van der Waals-Zeeman Instituut
Daily supervisors: J.C. Rouwhorst and S. Stuij
First reviewer: P. Schall
Second reviewer: D. Bonn

August 9, 2016



UNIVERSITEIT VAN AMSTERDAM

Abstract

The ageing of out of equilibrium systems, like colloidal gels, is of interest for scientific purposes and commercial applications, since they are present in many food products and personal care products. We investigated the ageing of colloidal gels at low effective particle interaction strength using a density matched system of PNIPAM particles suspended in a binary liquid of water and 2,6 Lutedine. The effective particle interaction strength is tunable by changing the temperature due to Critical Casimir forces. When the temperature approaches the phase separation temperature (T_s), the Critical Casimir force arises from the confinement of concentration fluctuations in the binary liquid. Confocal microscopy was used to capture images of the particles with a resolution large enough to locate individual particles. First we increased the temperature to high effective particle interaction strength until a gel was formed. After a gel was formed, the temperature was decreased in order to minimise the attractive force, meaning that bonds can break and the gel can restructure. Two measurements were performed at different interaction strength, where the restructuring is quantified by determining the connectivity of the particles, the center to center distance between connected particles and the fractal dimension from the structure factor. When the effective particle interactions is decreased it is seen that arms of the network will change to a more compact structure. When the effective particle interactions is pushed to the really low limit, it is seen that even bonds between previously connected particles can break. In conclusion, the gel will move towards a more connected structure with a higher fractal dimension.

Populair wetenschappelijke samenvatting

In mijn project heb ik onderzoek gedaan naar colloidal gels. Colloïden zijn deeltjes ter grootte van $1\text{ nm} - 10\text{ }\mu\text{m}$. Colloidal gels zijn te vinden in tandpasta, voedselproducten, gestold bloed en nog veel meer materie. Als we goed kunnen begrijpen welke natuurkunde er achter systemen met colloidal gels ligt, dan kan dit worden toegepast door bijvoorbeeld tandpasta harder of zachter te kunnen maken.

Bekend zijn de drie fases (toestanden); vaste stof, vloeistof en gas. Een gel zit tussen een vaste stof en een vloeistof in en wordt ook wel een halfvaste stof genoemd. Colloïden zijn vaste deeltjes die zijn gesuspendeerd in een vloeistof. Als colloïden aangetrokken zijn tot elkaar dan kunnen ze verbindingen met andere colloïden vormen. Zo kan er een netwerk (gel) ontstaan, zoals te zien is in figuur 1. Gels zijn systemen met een laag volumepercentage vaste deeltjes. Toch kunnen deze gels weerstand bieden en hun vorm behouden. Zo is er bekend dat gestold bloed kan onstaan met maar 0.1 volumepercentage vaste deeltjes.

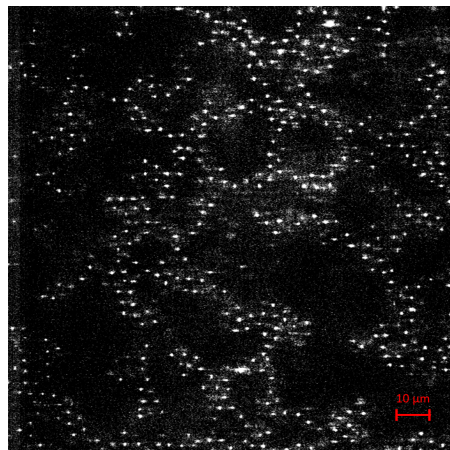


Figure 1: Een colloidal gel. Waarbij de verlichte punten de deeltjes zijn. Er is een willekeurige structuur waarbij allemaal vertakkingen zijn.

Op het moment dat er een gel gevormd wordt, is het systeem uit evenwicht. Dit betekent dat het systeem de neiging heeft om te veranderen zolang er geen evenwicht is. Door de sterkte tussen de interactie van Colloïden aan te passen, kan de mate van de verandering beïnvloed worden. De sterkte tussen de verbindingen kunnen we aanpassen met behulp van de klassieke variant van de Casimir krachten, die de Nederlandse professor Hendrik Casimir heeft ontdekt.

Met toepassing van Critical Casimir krachten zorg ik dat de sterkte tussen de Colloïden zo klein mogelijk is terwijl de gel niet uit elkaar valt. Doordat er zwakke verbindingen tussen colloïden zijn, hoop ik te kunnen zien dat verbindingen tussen colloïden kunnen verbreken. Deze deeltjes kunnen ergens anders in de gel weer verbonden raken.

Het is gelukt om verbindingen tussen colloïden te verbreken terwijl de rest van de structuur verbonden bleef. Om zichtbaar te maken welke veranderingen in de structuur plaatsvinden heb ik gekeken naar hoeveel verbindingen per colloid er zijn en hoe groot de afstanden afstanden zijn. Zichtbaar is dat de het aantal verbindingen per colloïde meer wordt in de tijd en dat de afstand tussen verbonden colloïden groter word. Mijn conclusie is dat de gel naar een dichter verbonden structuur gaat als verbindingen tussen colloïden verbroken kunnen worden.

Contents

1	Introduction	5
2	Theory	5
2.1	Colloidal gels	5
2.2	Critical Casimir force	6
2.3	Fractal Dimension	7
3	Method	8
3.1	Preparation of the samples	8
3.2	Measurements	8
3.3	Excitation and imaging	9
3.4	Data analysis	9
4	Results	11
4.1	Connectivity	14
4.2	Structure factor	17
5	Discussion	18
6	Conclusion	19
	References	19

1 Introduction

Colloids are all around us. From polluted rivers to volcanic ash, from hair gel to toothpaste and even in a lot of food products such as butter and cheese^{1,2}. An understanding of the physics behind colloids contributes in the research of the assembly of new functional materials.

In this paper we will be investigating the ageing of colloidal gels at weak effective particle interaction forces using confocal microscopy. When the inter-particle interaction between colloids is attractive, colloids can aggregate, forming space-spanning networks. These non-equilibrium systems are called gels. The physics behind colloidal gels is still largely unclear. Experiments of the ageing of gels have been done before where they quantified the restructuring of colloidal gels with scattering experiments³.

These colloidal particles are suspended in a binary liquid of water and Lutidine, meaning that we can tune the strength of the Critical Casimir force by changing the temperature. This way we can change the effective particle interaction strength. The temperature can continuously be changed throughout the measurement making the systems interaction strength tunable and the aggregation reversible⁴.

When the temperature is raised close to the critical temperature of the binary liquid, T_s , the Critical Casimir force will induce an effective particle interaction strength. The colloids will become attractive to each other and can start to aggregate. The temperature when this starts to happen is called the aggregation temperature T_a . To be able to see restructuring after the network was formed, the temperature was decreased to decrease the particle interaction strength. In this research the restructuring of 3-Dimensional gels will be quantified by determining the amounts of bonds per particle, the distance between those particles and calculating the fractal dimension from the structure factor for two different effective particle interaction strengths.

2 Theory

2.1 Colloidal gels

The word colloid, originally introduced by a Scottish scientist Thomas Graham, is derived from the Greek word Kolla ($K\delta\lambda\alpha$) and means glue. Colloids are particles that are of a specific size to exhibit Brownian motion. The diameter of colloids typically ranges from 0.01 till 10 μm ⁵. This means that colloids one larger dimension than atoms making imaging with confocal microscopy possible down to the level of single-particle resolution⁶.

When the effective inter-particle interaction of the colloids are attractive, they can start to aggregate and form a space spanning network known as a gel - "A semi-solid colloidal system consisting of a solid dispersed in a liquid"⁷. A gel can hold its shape and show elastic properties, despite its low volume fraction. For example coagulated blood with a volume fraction of only 0.1% solid material⁸.

The most attractive force in colloidal gels is the van der Waals force⁵. The van der Waals force is short-ranged. It arises from electrons motion in the two molecules. Electrons circle around the nuclei and create instantaneous dipoles¹. The averaged quantum fluctuations of the electric dipoles on the surface of the particle create an attractive force⁹. Frits London first analysed intermolecular interactions, so this force is also called the London dispersion interaction.

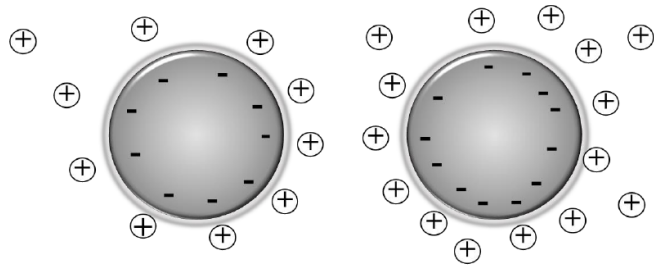


Figure 2: The dissolved Kalium ions surround the colloidal particles (large spheres) in suspension, which give rise to screening of the long range electrostatic interaction⁹.

The most important repellent force is the Coulomb force. The Coulomb force is due to charged surfaces^{10,11}. Adding KCl to the binary liquid decreases the range of the Coulomb force¹². KCl will dissolve in the binary mixture of water and Lutedine, leaving negative and positive ions in the mixture. The dissolved ions will surround the colloids as is visible in figure 2 screening the electrostatic repulsion⁹. This gives rise to screening of the long range electrostatic interaction, making the effective inter-particle attraction larger and therefore the colloids more attracted to each other.

2.2 Critical Casimir force

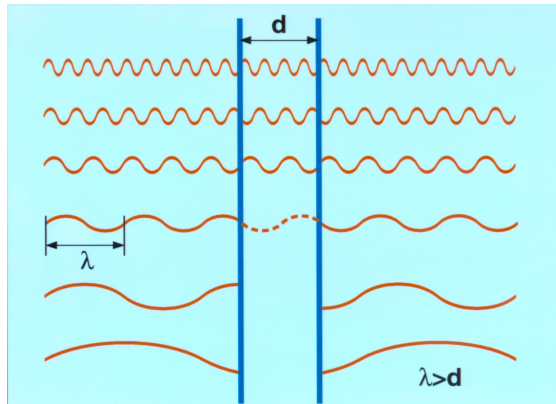


Figure 3: Fluctuations are bound between to parallel conducting plates

The first theoretical discovery of the quantum Casimir effect was in 1948 by Hendrik Casimir¹³. He concluded that, when the separation between the plates is small, there is an attractive force between two parallel, conducting and uncharged metal plates. This is because the fluctuations between the plates are bound. Only waves with a certain wavelength could fit within the plates, namely a wavelength of

$$\lambda = \frac{2 * d}{n} \quad (1)$$

in which d is the separation distance between the two plates and $n \in N$. Outside the plates bigger wavelengths can exist. An example of this is visible in figure 3. When you place two

parallel, conducting and uncharged metal plates close to each other, the fluctuations spectrum becomes reduced, resulting in a lower pressure between the plates, making it look like the plates are attractive to each other and pushing them closer together.

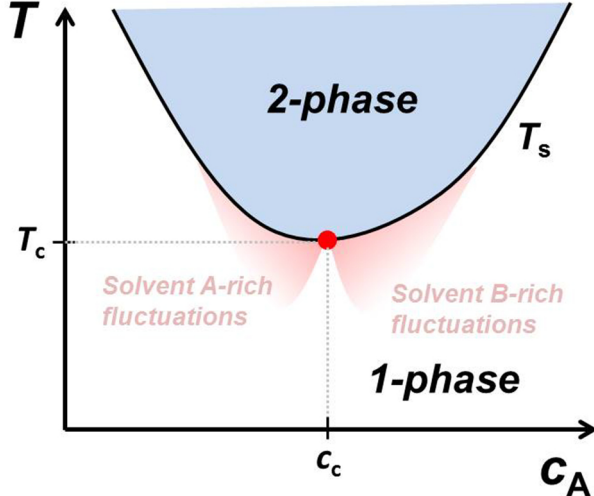


Figure 4: Schematic phase diagram of a binary solvent of water and 2,6 Lutidine¹⁴. In our case we are on the left with water rich fluctuations. were T_s is the critical temperature were you increase the temperature shift from the homogeneous phase 1 to the the separated phase 2. The red region shows the range of aggregation were solvent fluctuations grow upon approaching the critical point.

A similar effect happens in its classical analog, the Critical Casimir effect. In figure 4 you see a schematic phase diagram of the binary liquid of water and Lutedine. It shows phase 1 where the two liquid components mix uniformly and phase 2 where the liquids separate. When starting from phase 1 and raising the temperature close to the phase separation line T_s , concentration fluctuations appear in the liquid. The confinement of those solvent concentration fluctuations between the surfaces of neighbouring particles leads to an attraction force between the particles.

2.3 Fractal Dimension

Lines are one-dimensional, surfaces are two-dimensional and volumes are three dimensional. A line segment can be broken in N self-similar pieces, each with a magnification factor M. The fractal dimension is the exponent of the number of self-similar pieces with magnification factor M into which the figure may be broken. Thus, we can write the fractal dimension as follows;

$$D_f = \frac{\log(\text{Number of self-similar pieces})}{\log(\text{Magnification factor})} \quad (2)$$

with D_f the fractal dimension. An ideal fractal is a self-similar geometric object, which is infinitely complicated. A geometric figure is self-similar, if there is a point where every zoomed in or zoomed out version contains a copy of the entire figure. This self-similarity can be calculated from the structure factor. The structure factor will show the characteristic structure of the gel. The slopes of the structure factor in log - log coordinates define the differential fractal dimension^{15,16} as

$$S(q) = A * q^{-D_f}. \quad (3)$$

In equation 3, $S(q)$ are the linear parts of the structure factor in log scale, A is a constant and D_f is the fractal dimension.

3 Method

To look at ageing of a gel in 3 dimensions, a line-scanning confocal microscope has been used. Colloidal particles were suspended in binary liquid of water and Lutidine. In order to see the particles with confocal microscopy, the sample has to be prepared.

3.1 Preparation of the samples

For the measurements Poly N-isopropylacrylamide, (PNIPAM) particles were used. The PNIPAM particles are dyed with Rhodamine to be able to observe them with confocal microscopy. For the measurements the dyed PNIPAM particles were dissolved in a binary liquid. This binary liquid contains 27 wt % Lutidine and 73 wt % water. It also has a concentration of 30 mM KCl.

There is still a lot of dye floating around in the sample, since the particles were suspended in a dye. To remove remaining dye, the sample has been washed by centrifuging. The particles were centrifuged at 3000g and a temperature of 20°C for one hour. After the centrifuging, the sample was separated with on the bottom the colloidal particles and on top the binary liquid. As much binary liquid as possible was removed without removing the colloidal particles. After the binary liquid has been removed, new binary liquid was added until the total weight was similar as before. This process was repeated four times.

To be able to do measurements with the sample, around 30 μL of the sample has been pipetted in two capillaries. An example of a capillary can be seen in figure 5. Both ends of the capillary have been closed by filling it with Teflon paste and pouring glue over the ending sides.

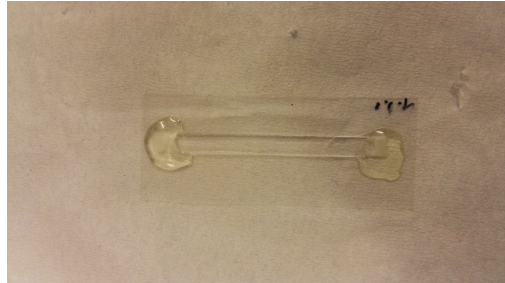


Figure 5: Capillary used to conduct the measurements.

3.2 Measurements

Two measurements were done for two capillaries with the sample. First a gel was created by increasing the temperature close to T_s . For both measurements, the temperature was increased to 32.00(1)°C and kept constant for 10 minutes. To see restructuring after the gel was formed, the temperature was decreased to decrease the effective particle interaction strength. For one measurement the temperature was decreased to 31.00(1)°C and for the other to 30.35(1)°C. After this decrease, the restructuring of the gel was measured for 13.2 hours keeping the temperature constant.

3.3 Excitation and imaging

The measurements were done using a line-scanning confocal microscope to acquire images with a volume of $105\mu m * 105\mu m * 28\mu m$, at a rate of 6 images per hour. The captured images were taken with a resolution of 1024 by 1024 pixels and, a dept of 12 bits. The used line laser had a wavelength of 532nm. For a line scanner only one rotating mirror is needed to create a full 2D image. The light that comes from the line scanner hits the rotating mirror and goes through the dichroic mirror. Light with a certain wavelength will go through while light with other wavelengths will be reflected. After the dichroic mirror, the light will go through the objective. An oil immersion objective was used to optimally increase the numerical aperture. After the objective, the light excites the dye of the particles in a certain layer of the sample. When the dye relaxes back to the ground state, it will emit light with lower energy and therefore light with a longer wavelength. This is also known as fluorescence. The emitted light will go through the objective and is reflected by the dichroic mirror to the longpass filter. This filter will filter all light below 550nm to make sure only light coming from the dye on the particles is visible. This also prevents the light from the 532nm line laser.

It is also possible that the light hits the dye on a particle in another layer of the sample. This light from a different layer hits the dichroic mirror at a different angle. To prevent this light from being detected, a pinhole is placed in front of the detector filtering all incoming light with a different angle than the light coming from the measured layer. In order to create 3D images, the sample is moved up and down. Combining the multiple 2D slices, a 3D image is created. The schematic view of the setup can be seen in figure 6.

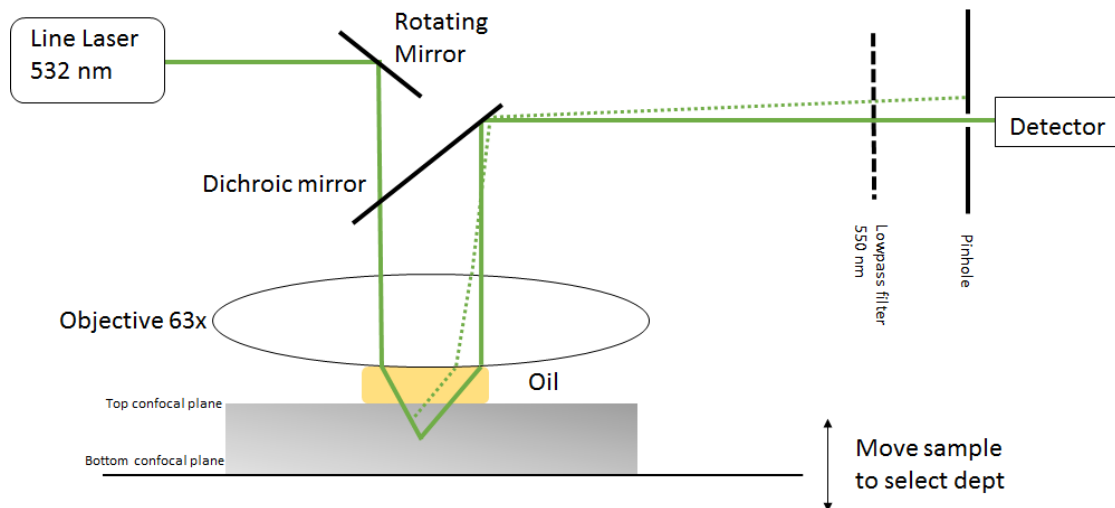


Figure 6: Schematic view of the line-scanning confocal microscope that is used in this experiment.

3.4 Data analysis

The raw image from the confocal microscope was bandpass filtered, filtering the noise up to 2 pixels thick and smoothing particles down to 10 pixels, effectively removing background noise. These bandpass parameters were determined by looking at the image. To minimise the influence of bleaching throughout the measurement, the image was normalised for each time frame.

After the image was pre-processed, the particles were located in 3-Dimensions using a locating

algorithm¹⁷. When a histogram of the total intensity of the found particles is plotted, there will be two peaks. The lowest intensity peak is small in width and is noise. The second peak represents the particles. The difference in the total intensity (mass) from located particles can be seen in figure 7a, where the first peak (blue) is the noise and the second peak (green) are the particles. In order to remove additional noise, the minimum between the peaks was determined and everything before this minimum was deleted. To check whether this is a good fit, the identified particles locations are put on top of the real image as can be seen in figure 7b. We do not observe any noise and we appear to not miss any particles.

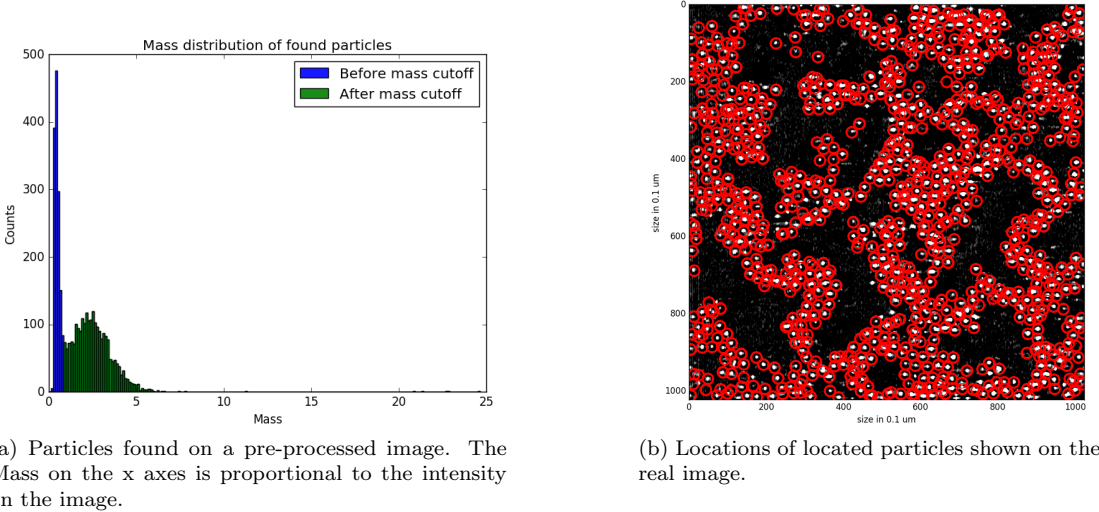


Figure 7: To optimise the locating of particles and remove noise, all the located particles before the minimum between the first peak and the second peak in are deleted.

When all particles were located, the connectivity between the particles was determined by using a threshold distance of $3.5 \mu\text{m}$ to define bonded particles. This means that we consider two particles are connected if they are within a radius of $3.5 \mu\text{m}$ from each other. After this the center to center distance between connected particles was determined. From these distances a histogram was made. Since the distance between connected particles is approximately a Gaussian distribution, a Gaussian fit was done on the data in the histogram to determine the expected value of the center to center distance between connected particles.

We also determined the structure factor using the raw image obtained from the confocal microscope. Since the structure factor is the angle average of the Fourier transformed image, the raw image was first Fourier transformed using Fast Fourier transformation. Then the origin of the images is shifted to the center of the image to calculate the angle average. The angle average was calculated by summing over the intensity of all pixels within a circle of radius q to $q + dq$ and dividing by the total amount of pixels within that circle as can be seen in figure 8. This was done until the maximum radius of which the circle still fully fitted in the image. Thus, q values larger than the width of the image were neglected. In the real image, the radius can also not be larger than the width of size of the image. The smallest length scales of the Fourier transformed image correspond to the largest length scales in the real space image. The structure factor $S(q)$ is then plotted in log - log scale from which the fractal dimensions were fitted of the linear parts of the curve using equation 3.

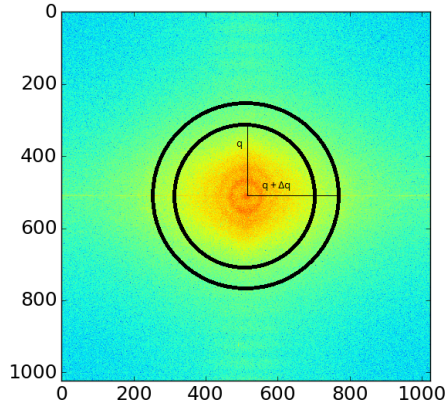


Figure 8: Example of a Fourier transformed image using fast Fourier transformation.

4 Results

When the temperature is far below T_s we observe that the colloids move around in random directions. Particles do not stick together. Hence we start with a homogeneously distributed sample as can be seen in figure 9. When the temperature is raised too high, above T_s , the binary mixture will phase separate and small droplets containing colloids will form as can be seen in figure 10.

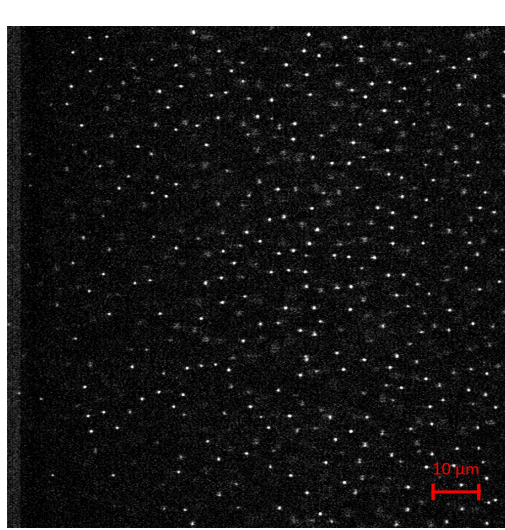


Figure 9: An image far below T_a where no gel is yet formed.

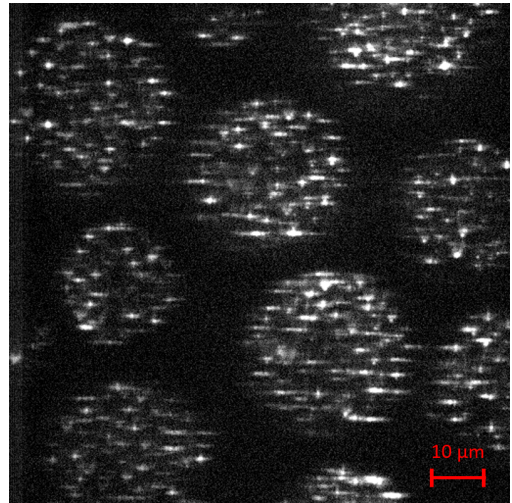


Figure 10: An image above T_s where the binary liquid is phase separated and the gel is destroyed.

However, when we heat the sample the temperature just below T_s , particles aggregate and eventually form a space-filling network. We investigated the ageing of the network at two different temperatures $T_1 = 31.00(1)^\circ C$ and $T_2 = 30.35(1)^\circ C$, corresponding to different particle interactions. Snapshots of the particles taken during the ageing experiments are shown in figure

11 and 12, respectively.

Both measurements show an observable change in the structure at the beginning of the experiment, while later much less restructuring happens. With the measurement of $31.00(1)^\circ\text{C}$ we only observe the shifting of the filaments of the network and some vibrations in the gel. With the measurement of $30.35(1)^\circ\text{C}$ much more happens. The same shifting of the filaments of the network is seen, but also bonds between connected particles can break. Particles can be seen moving throughout the sample during the entire measurement.

When figure 11a is compared with figure 11b one can see that at $30.35(1)^\circ\text{C}$ much more restructuring is observed. The filaments appear to thicken and move to a more compact structure in time. When inspecting the measurement of $31.00(1)^\circ\text{C}$ we observe that bonds do not break. This is confirmed when figure 11b is compared with figure 11c. No significant restructuring takes place when the filaments stop shifting. The latest taken image is of low quality due to bleaching, as can be seen in figure 11d.

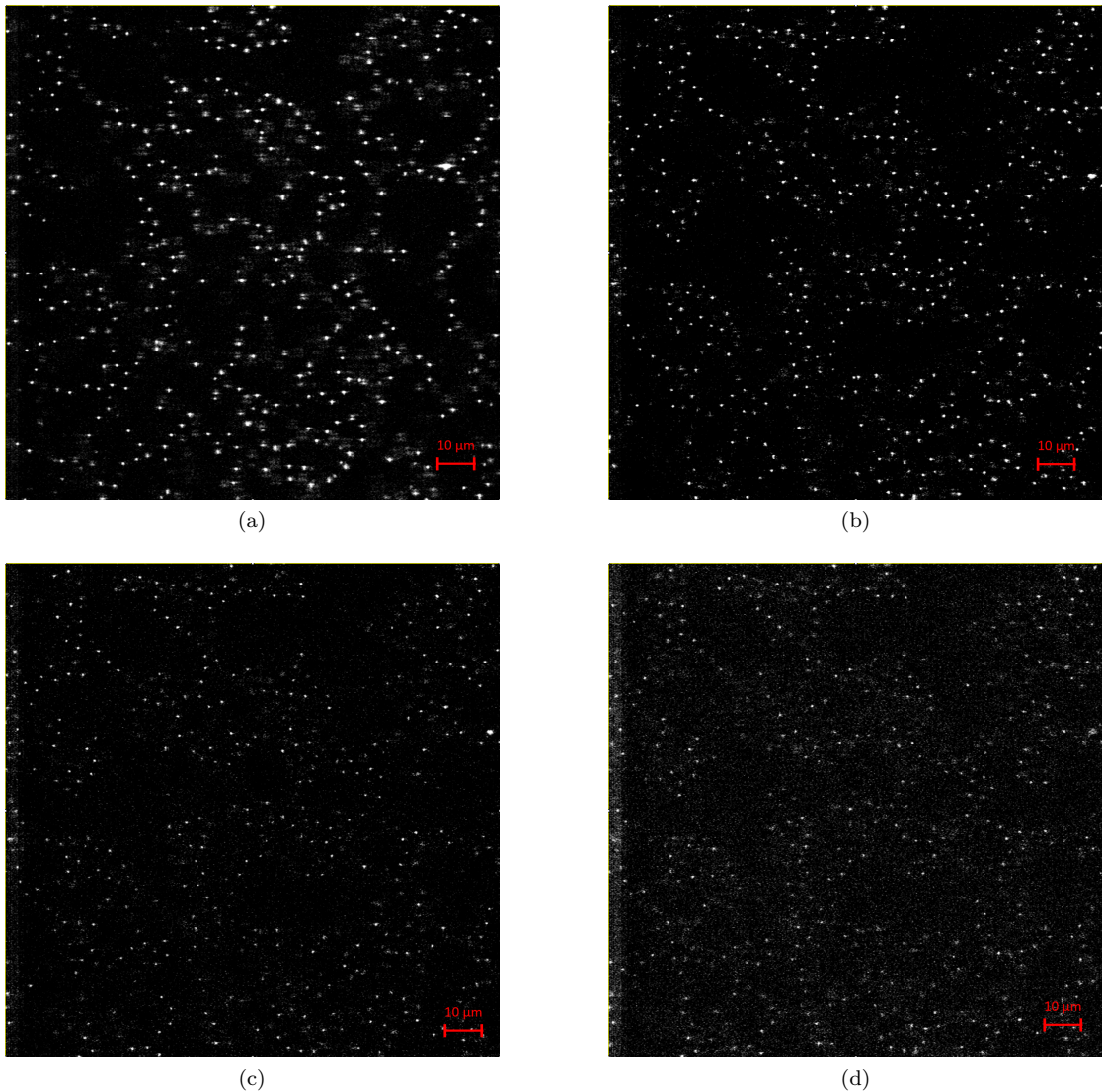


Figure 11: Confocal microscope images, taken at the same location in the sample at the start of the measurement (a), after 5 hours (b), after 10.8 hours(c) and after 13.2 hours (d) at a temperature of $31.00(1)^\circ\text{C}$.

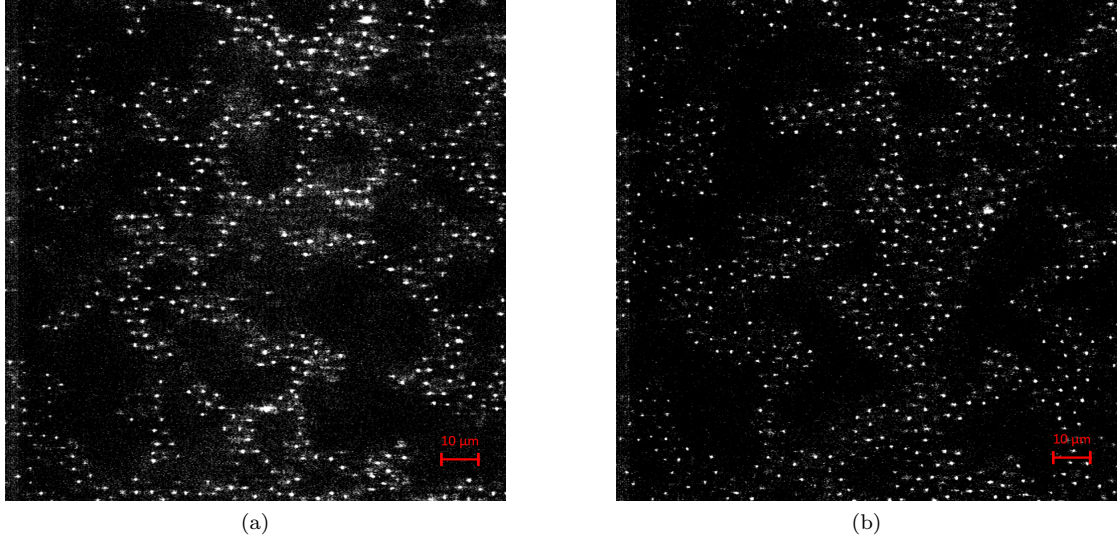


Figure 12: Confocal microscope images, taken at the same location in the sample at the start of the measurement (a) and after 13.2 hours (b) at a temperature of $30.35(1)^\circ\text{C}$.

4.1 Connectivity

From the located particles we determined the connectivity using the $3.5 \mu\text{m}$ threshold. The determined number of bonds per particle is displayed in figure 13 and 14. In the beginning, there is a significant change in the number of bonds per particle. After that, the number of bonds saturates. In figure 13 you can see that the percentage of particles with 1 to 3 bonds decreases, while the percentage of particles with 4 to 6 bonds increases. In figure 14 on the other hand, the percentage of particles with 3 to 5 bonds decreases, while the percentage of particles with 7 to 9 bonds increases. This increase in neighbours indicates that the gel forms towards a more bonded structure.

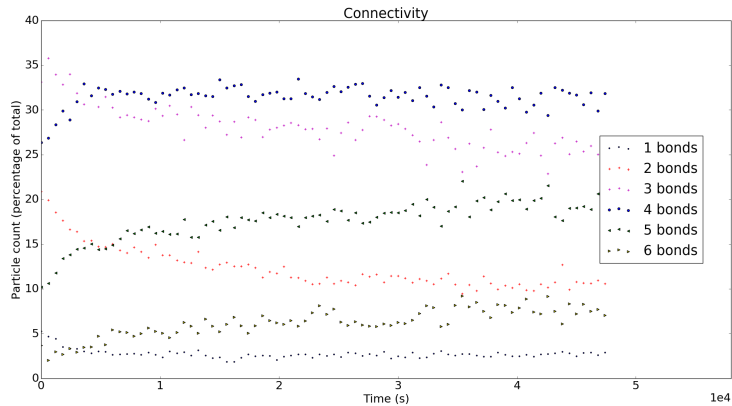


Figure 13: The percentage of the amount of particles with a specific amount of neighbours. Determined by setting a threshold of $3.5\mu\text{m}$ on all the located particles. Measurement of $31.00(1)^\circ\text{C}$.

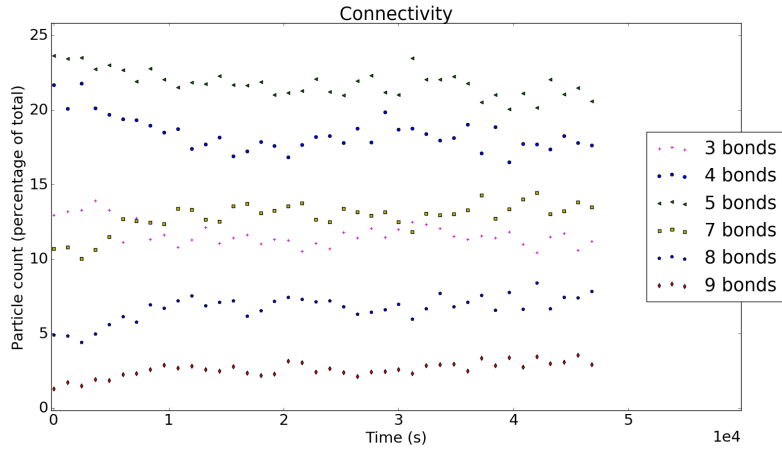


Figure 14: The percentage of the amount of particles with a specific amount of neighbours. Determined by setting a threshold of $3.5 \mu m$ on all the located particles. Measurement of $30.35(1)^\circ C$.

As you can see in figure 15 the number of particles increases with time. This is due gravity. Particles from layers above will sediment to form denser structure close to the bottom of the cell.

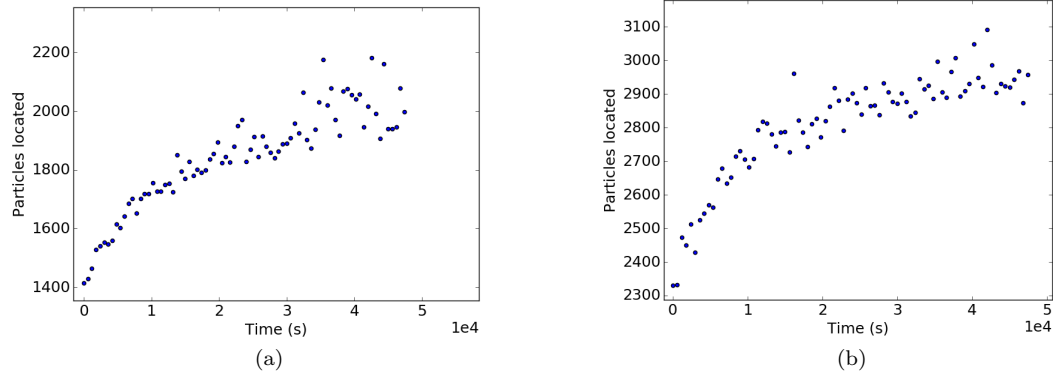


Figure 15: Particles found. Measurement of $31.00^\circ C$ (a) and $30.35^\circ C$ (b)

In figure 16 the center to center distance are shown for the first frame and the last frame for both measurements. In both figures it is visible that the counts increases. Thus, there are more particles with bonds. In figure 16b it is also seen that the counts mainly increases on the large center to center distance length scale.

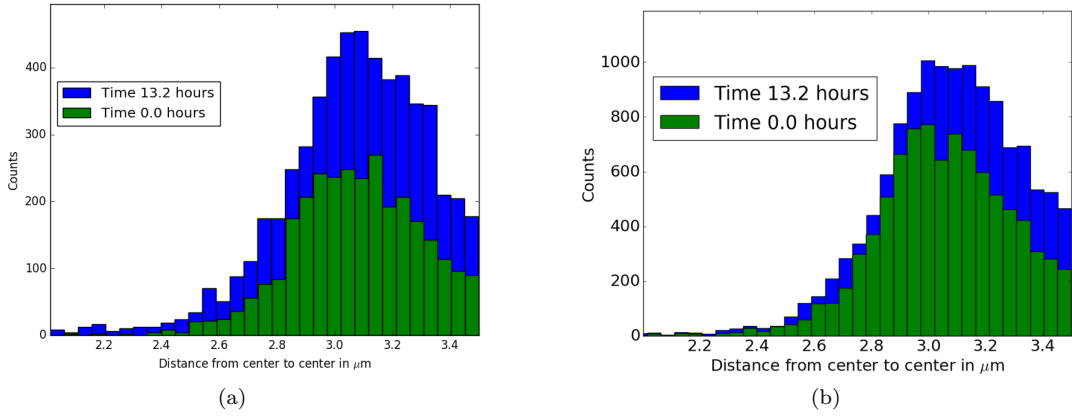


Figure 16: Un-normalised histogram of the center to center distance between connected particles.
 (a) Measurement of $31.00(1)^\circ\text{C}$ and (b) Measurement of $30.35(1)^\circ\text{C}$.

In figure 17 we show the mean center-to-center distance determined from the Gaussian fit using of the data of figure 16. There is a big increase in count visible, this increase is possible due to sedimentation. In figure 17b there is a systematic increase in the distance from center to center in connected particles from $3.11(1) \mu\text{m}$ to $3.13(1) \mu\text{m}$ and in figure 17a an increase from $3.12(1) \mu\text{m}$ to $3.14(1) \mu\text{m}$.

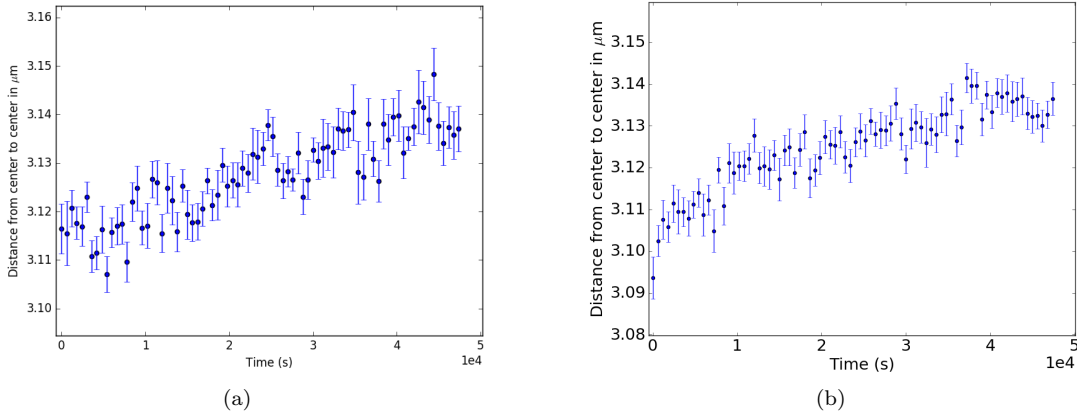


Figure 17: Plotted peaks of the distance histogram. Found by plotting a Gaussian on the histogram of figure16. (a) Measurement 1 of $31.00(1)^\circ\text{C}$, (b) Measurement 2 of $30.35(1)^\circ\text{C}$.

4.2 Structure factor

The structure factor $S(q)$, calculated from the angle average of the Fourier transformed image, is shown in figure 18. There are four peaks visible in both structure factors. In both cases, the positions of these peaks do not shift significantly in time. It is visible that the slope of the linear parts of the structure factor in log-log scale change in time.

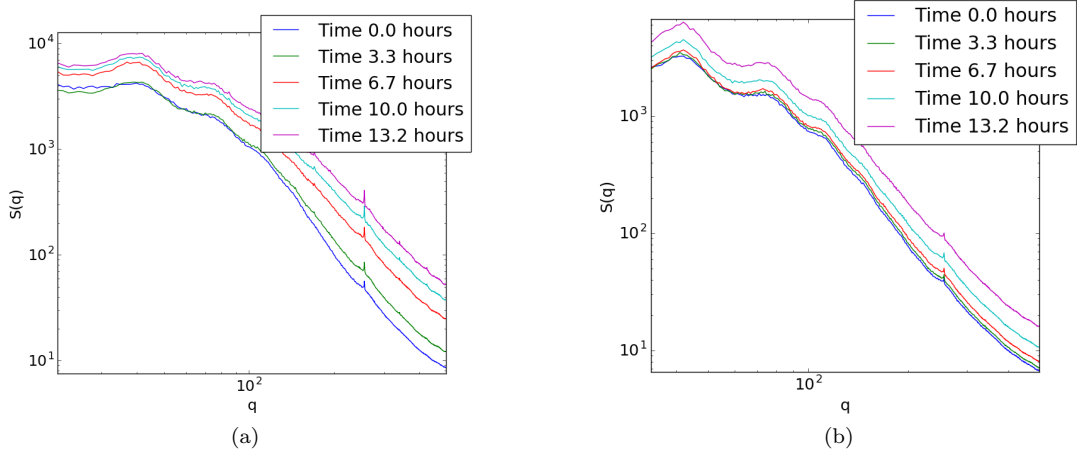


Figure 18: Structure factor obtained by Fourier transformation of the real-space images. (a) Ageing Measurement at $31.00(1)^\circ\text{C}$, (b) Measurement at $30.35(1)^\circ\text{C}$.

From the linear parts of the curve, the fractal dimension has been determined using equation 3. The fractal dimensions found can be seen in figure 19. For high particle interaction strength, fractal dimension is low. At short times it increases rapidly, while at longer times it decreases slowly. In contrast to the fractal dimension at low interaction strength is higher and keeps increasing throughout the measurement to a fractal dimension of almost 3. This shows that the structure continuously becomes more compact during the ageing.

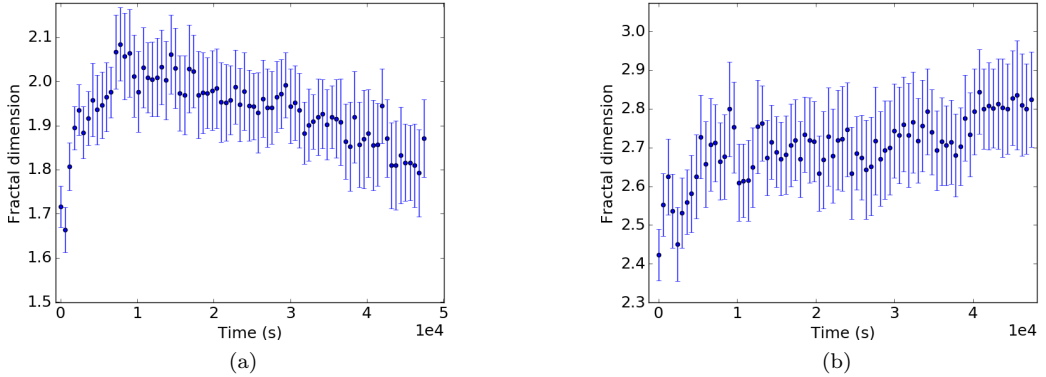


Figure 19: The fractal dimension fitted from the slope of the linear parts of the curve from figure 18. (a) Measurement 1 of $31.00(1)^\circ\text{C}$, (b) Measurement 2 of $30.35(1)^\circ\text{C}$.

5 Discussion

What is seen on the raw data is confirmed by results for the connectivity. In the image it is visible that filaments get bigger and thus particles will have more neighbours. In figure 14 and figure 13 you can see that the number of bonds per particle increases for both measurements. Since there is not much restructuring happening after the beginning we would expect less bonds change in time for the measurement of 31.00°C , however we do still see some change. This can be attributed to bleaching effects we can observe in figure 11d.

In figure 17, you can clearly see a systematic shift of the peaks of the center to center distance between connected particles. This could indicate that the ageing of the gel increases the separation distance between particles. Since the depth of the interaction potential has been decreased rather quickly, this increase cannot be a direct effect of the Critical Casimir force. This can happen because particles will get more neighbours and thus be pulled outwards by the inter-particle interactions increasing the distance between the connected particles. Another reason could be that the threshold is too large and we found particle connections that do not exist. The measurements should be repeated to see whether the right threshold is used and to confirm the reason for the increase in the separation distance between connected particles.

When calculating the fractal dimensions we see a big change between the two measurements. In figure 19b we can see a steady increase in fractal dimension, while in figure 19a we see first that the fractal dimension increases and then decreases. The steady increase of the fractal dimension of the measurement of $30.35(1)^\circ\text{C}$ corresponds with what we would expect, since we can see bonds break on the real-image throughout the whole measurement indicating restructuring. We also see a difference in the beginning value of the fractal dimension, while it is the same system. This is because we started the sample of 31.00°C with a less dense structure. There are around 40% less particles in the measurement of 31.00°C as can be seen in figure 15.

The amount of particles increases in time due to gravity. This effect of gravity will also influence the ageing, but it is difficult to avoid on these long-time measurements. Experiments in microgravity habitats are required to be sure to cancel out any effect of gravity.

6 Conclusion

In conclusion we have investigated the ageing of a 3 dimensional gel by quantifying the amount of bonds per particle, the distance between those particles and calculating the fractal dimension from the structure factor for two different effective particle interaction strength.

When the effective particle interactions are decreased filaments of the network will change to a more compact structure. When the effective particle interactions is pushed to the really low limit, even bonds between previously connected particles can break. From the data it is visible that the amount of connected particles increases and the distances between the connected particles increases as well for both particle interaction strengths. Finally, the fractal dimension increases to a volume of almost 3 for low interaction strengths, while for higher interaction strengths the fractal dimension stabilises at a much lower fractal dimension. The whole process, however, may be affected by gravity as we see the number of particles increase over time, indicating sedimentation.

Because gravity will always have influence on the restructuring of the gel, follow-up experiments should be done under microgravity conditions. Additionally, these measurements should be repeated using even lower effective particle interaction strengths.

References

- 1 Evans DF, Wennerström H. The Colloidal Domain: Where Physics, Chemistry, Biology, and Technology Meet. Advances in Interfacial Engineering. Wiley; 1999. Available from: <https://books.google.nl/books?id=XPjvAAAAMAAJ>.
- 2 Dinsmore AD, Yodh AG, Pine DJ. Phase diagrams of nearly-hard-sphere binary colloids. *Phys Rev E*. 1995 Oct;52:4045–4057. Available from: <http://link.aps.org/doi/10.1103/PhysRevE.52.4045>.
- 3 Cipelletti L, Manley S, Ball R, Weitz D. Universal aging features in the restructuring of fractal colloidal gels. *Physical review letters*. 2000;84(10):2275.
- 4 Veen SJ, Antoniuk O, Weber B, Potenza MA, Mazzoni S, Schall P, et al. Colloidal aggregation in microgravity by critical Casimir forces. *Physical review letters*. 2012;109(24):248302.
- 5 Weeks ER. Soft jammed materials. ER Maruyama, S & Tokuyama, M(Eds), *Statistical Physics of Complex Fluids*. 2007;p. 243–255.
- 6 Prasad V, Semwogerere D, Weeks ER. Confocal microscopy of colloids. *Journal of Physics: Condensed Matter*. 2007;19(11):113102.
- 7 Dictionary OE. Oxford English dictionary online. 2016;.
- 8 Cianci G, Hunter G, Samphel T, Soo T, Weeks E. *Colloidal Gels and Depletion*;.
- 9 López-Esparza R, Altamirano B, Pérez E, Gama Goicochea A. Importance of molecular interactions in colloidal dispersions. *Advances in Condensed Matter Physics*. 2015;2015.
- 10 Larson RG. The Structure and Rheology of Complex Fluids. Topics in Chemical Engineering. OUP USA; 1999. Available from: https://books.google.de/books?id=Vt9fw_pf1LUC.
- 11 Jones RA. Soft condensed matter. vol. 6. Oxford University Press; 2002.

- 12 Yethiraj A, van Blaaderen A. A colloidal model system with an interaction tunable from hard sphere to soft and dipolar. *Nature*. 2003;421(6922):513–517.
- 13 Casimir HB. On the attraction between two perfectly conducting plates. In: Proceedings of the KNAW. vol. 51; 1948. p. 793–795.
- 14 Nguyen V, Dang M, Nguyen T, Schall P. Critical Casimir forces for colloidal assembly. *Journal of Physics: Condensed Matter*. 2016;28(4):043001.
- 15 Müller M, Wittmer J, Cates M. Topological effects in ring polymers. II. Influence of persistence length. *Physical Review E*. 2000;61(4):4078.
- 16 Mokhtari T. Studies of the effects of shear on colloidal aggregation and gelation using small angle light scattering. ProQuest; 2007.
- 17 Allan D, Caswell T, Keim N, van der Wel C. trackpy: Trackpy v0.3.0; 2015. Full list of contributors: Aron Ahmadia, Continuum Analytics; Franois Boulogne, Princeton University; Rebecca Perry, Harvard University; Al Piszcza, The Mitre Corporation Jan Schulz, TU Freiberg; Leonardo Uieda, Universidade do Estado do Rio de Janeiro. Available from: <http://dx.doi.org/10.5281/zenodo.34028>.